УДК 616.831-073.756.8-073.86
https://doi.org/10.20538/1682-0363-2021-2-191-201

Diffusion magnetic resonance imaging data: development of methods and tools for diagnosis and treatment of brain diseases

Urazova K.A.[1, 3], Gorlachev G.E.[2], Chernyaev A.P.[3], Golanov A.V.[1]

[1] N.N. Burdenko National Scientific and Practical Center for Neurosurgery
16, 4th Tverskaya-Yamskaya Str., Moscow, 125047, Russian Federation

[2] N.N. Blokhin National Medical Research Center of Oncology
24, Kashirskoye Highway, Moscow, 115478, Russian Federation

[3] M.V. Lomonosov Moscow State University
1, Leninskie Gory, Moscow, 119991, Russian Federation

ABSRACT

The use of quantitative mapping of diffusion characteristics carries great potential for diagnosis and therapy of brain diseases, since it potentially allows to classify tumors, determine the degree of their malignancy, differentiate various morphological structures of tumor and non-tumor pathologies (such as tumor stroma, necrotic zones, cysts, various types of edema, etc.), and predict the course and outcome of diseases, in particular, a clinical response to treatment. Based on diffusion weighted magnetic resonance imaging (MRI), it is possible to perform 3D modeling of the white matter pathways of the brain, which is called tractography. In addition to a unique ability to visualize the location of tracts in relation to intracranial pathologies, this technology allows to build and analyze complex maps of communication networks in the brain (connectomics).

The review is devoted to the discussion of the physical and technical concept of diffusion weighted MRI, the key ways of its application in tumor and non-tumor processes, and problems that complicate correct interpretation of results. Since the problem of developing software for diffusion MRI data remains relevant, this review presents our own experience in developing an application as part of the project on creating effective methods for processing diffusion MRI data and modeling white matter tracts.

Key words: magnetic resonance imaging, diffusion weighted magnetic resonance imaging, tractography, brain, neuroscience.

Conflict of interest. The authors declare the absence of obvious and potential conflicts of interest related to the publication of this article.

Source of financing. The study was supported by the Russian Foundation for Basic Research (project No. 19-32-90198).

For citation: Urazova K.A., Gorlachev G.E., Chernyaev A.P., Golanov A.V. Diffusion magnetic resonance imaging data: development of methods and tools for diagnosis and treatment of brain diseases. *Bulletin of Siberian Medicine.* 2021; 20 (2): 191–201. https://doi.org/10.20538/1682-0363-2021-2-191-201.

✉ *Urazova Ksenia A.,* e-mail: kurazova@nsi.ru.

Диффузионные данные магнитно-резонансной томографии: разработка методологии и инструментов использования в диагностике и лечении заболеваний головного мозга

Уразова К.А.[1, 3], Горлачёв Г.Е.[2], Черняев А.П.[3], Голанов А.В.[1]

[1] Научный медицинский исследовательский центр (НМИЦ) нейрохирургии имени академика Н.Н. Бурденко Россия, 125047, г. Москва, 4-я Тверская-Ямская ул., 16

[2] Научный медицинский исследовательский центр (НМИЦ) онкологии имени Н.Н. Блохина Россия, 115478, г. Москва, Каширское шоссе, 24

[3] Московский государственный университет (МГУ) имени М.В. Ломоносова Россия, 119991, г. Москва, Ленинские горы, 1/2

РЕЗЮМЕ

Использование различных карт количественных характеристик диффузии несет в себе большой потенциал для медицинской диагностики и терапии патологии головного мозга, так как позволяет классифицировать опухоли, определять степень их злокачественности, дифференцировать различные морфологические структуры опухолевых и неопухолевых патологических процессов (таких как строма опухоли, зоны некроза, кисты, различные виды отека и т.д.), прогнозировать течение и исход заболеваний, в частности клинический ответ на проведенное лечение. На основе диффузионно-взвешенной томографии возможна реализация трехмерной реконструкции волокон белого вещества головного мозга, называемая трактографией. Помимо уникальной возможности визуализировать расположение трактов относительно интракраниальных патологических изменений, данная технология позволяет строить и анализировать комплексные карты сложных сетей связей в головном мозге (коннектомика).

Обзор посвящен обсуждению физико-технической концепции диффузионно-взвешенной томографии, ключевых направлений применения в случае опухолевых и неопухолевых процессов, а также проблем, затрудняющих процесс корректной интерпретации результатов. Так как в настоящий момент остается актуальной задача применения программного обеспечения для работы с диффузионными показателями магнитно-резонансной томографии, то в представленном обзоре показан собственный опыт разработки приложения в рамках проекта по созданию эффективных методик интерпретации диффузионных данных и построению трактов белого вещества головного мозга.

Ключевые слова: магнитно-резонансная томография, диффузионно-взвешенная томография, трактография, головной мозг, нейронауки.

Конфликт интересов. Авторы декларируют отсутствие явных и потенциальных конфликтов интересов, связанных с публикацией настоящей статьи.

Источник финансирования. Исследование выполнено при финансовой поддержке Российского фонда фундаментальных исследований (проект № 19-32-90198).

Для цитирования: Уразова К.А., Горлачёв Г.Е., Черняев А.П., Голанов А.В. Диффузионные данные магнитно-резонансной томографии: разработка методологии и инструментов использования в диагностике и лечении заболеваний головного мозга. *Бюллетень сибирской медицины.* 2021; 20 (2): 191–201. https://doi.org/10.20538/1682-0363-2021-2-191-201.

INTRODUCTION

Introscopy is a key discipline in medical diagnostics. Technical advances in computed tomography machine design and software made it possible to solve existing problems and open up new scientific directions that previously could not be invasively studied on people. In this context, diffusion weighted imaging (DWI) has become a widely used technique for studying the structure and functions of the brain, since it allows to measure the orientation of white matter fibers *in vivo*. This is especially relevant in the fields of stereotactic radiosurgery and neurosurgery, where it is important to measure the degree of involvement of functionally significant areas in the pathological process, while in certain cases, the

standard set of images (T1-weighted (T1w), T1w contrast-enhanced, T2-weighted (T2w), fluid-attenuated inversion recovery (FLAIR) images, etc.) may not be enough to differentiate various morphological structures in tumor and non-tumor pathological processes.

PHYSICAL AND TECHNICAL FEATURES OF DIFFUSION MRI DATA

DWI is a technique of magnetic resonance imaging (MRI) that provides information about microscopic displacements of water molecules that occurs in biological tissues due to physical diffusion.

Vector $\mathbf{r}_0$ is the initial position of the particle at $t = 0$, and vector $\mathbf{r}$ is its subsequent position at $t = \tau$. Generalizing the Einstein's equation [1] to the case of an anisotropic medium, we obtain:

$$D = \frac{1}{6\tau}\langle \mathbf{R}^T \cdot \mathbf{R} \rangle = \begin{bmatrix} Dxx & Dxy & Dxz \\ Dyx & Dyy & Dyz \\ Dzx & Dzy & Dzz \end{bmatrix}, \quad (1)$$

where D is the diffusion tensor, and the vector $\mathbf{R} = \mathbf{r}\text{-}\mathbf{r}_0$ shows particle displacement. It can be shown that this second-rank tensor is symmetric and positive definite, and that its eigenvalues are real.

It is necessary to obtain several DWI in different noncollinear directions of the gradient g_k ($k = 1, ..., N$) to calculate the diffusion tensor D($\mathbf{r}$) [2]. In general, the diffusion tensor can be calculated by solving the following system of equations:

$$S_k(\mathbf{r}) = S_0(\mathbf{r}) e^{-b\hat{g}_k^T \cdot D(\mathbf{r}) \cdot \hat{g}_k}, \text{ где } \hat{g}_k = \frac{g_k}{\|g_k\|}, \quad (2)$$

where $S_0(\mathbf{r})$ is the signal in the absence of diffusion gradients (i.e., $\|g\| = 0$).

Coefficient b is the so-called b-factor, introduced in [3] and defined as:

$$b_k = \gamma^2 \delta^2 \left(\Delta - \frac{\delta}{3}\right) \|g\|^2, \quad (3)$$

where γ is the gyromagnetic ratio of hydrogen (42.58 MHz / T), δ is the signal duration, and Δ is the time between the pulses.

The probability density function $p(\mathbf{r}|\mathbf{r}_0, \tau)$ for an anisotropic medium:

$$p(\mathbf{r} \,|\, \mathbf{r_0}, \tau) = \frac{1}{\sqrt{(4\pi\tau)^3 |D|}} e^{-\frac{(\mathbf{r}-\mathbf{r_0})^T \cdot D^{-1} \cdot (\mathbf{r}-\mathbf{r_0})}{4\tau}}, \quad (4)$$

Also, since the $\|g_k\|$ are different, the b-factor can be expressed as follows:

$$b_k = \gamma^2 \delta^2 (\Delta - \frac{\delta}{3}) \|g_k\|^2, \quad (5)$$

It is more convenient to rewrite the system of equations (2) in the form:

$$\begin{bmatrix} (\hat{g}_{1x})^2 & 2\hat{g}_{1x}\hat{g}_{1y} & 2\hat{g}_{1x}\hat{g}_{1z} & (\hat{g}_{1y})^2 & 2\hat{g}_{1y}\hat{g}_{1z} & (\hat{g}_{1z})^2 \\ (\hat{g}_{2x})^2 & 2\hat{g}_{2x}\hat{g}_{2y} & 2\hat{g}_{2x}\hat{g}_{2z} & (\hat{g}_{2y})^2 & 2\hat{g}_{2y}\hat{g}_{2z} & (\hat{g}_{2z})^2 \\ \vdots & \vdots & \vdots & \vdots & \vdots & \vdots \\ (\hat{g}_{Nx})^2 & 2\hat{g}_{Nx}\hat{g}_{Nz} & 2\hat{g}_{Nx}\hat{g}_{2N} & (\hat{g}_{Ny})^2 & 2\hat{g}_{Ny}\hat{g}_{Nz} & (\hat{g}_{Nz})^2 \end{bmatrix} \begin{bmatrix} D_{xx}(\mathbf{r}) \\ D_{xy}(\mathbf{r}) \\ D_{xz}(\mathbf{r}) \\ D_{yy}(\mathbf{r}) \\ D_{yz}(\mathbf{r}) \\ D_{zz}(\mathbf{r}) \end{bmatrix} = \begin{bmatrix} \frac{1}{b}\ln\frac{S_0(\mathbf{r})}{S_1(\mathbf{r})} \\ \frac{1}{b}\ln\frac{S_0(\mathbf{r})}{S_2(\mathbf{r})} \\ \vdots \\ \frac{1}{b}\ln\frac{S_0(\mathbf{r})}{S_N(\mathbf{r})} \end{bmatrix} \quad (6)$$

$$\mathrm{G} \qquad \widetilde{D(\mathbf{r})} \qquad \mathrm{B}(\mathbf{r})$$

If more than 6 directions are obtained, then the system of equations (6) can be solved using the least squares approximation. For example, if you use a linear unweighted least squares approximation, then:

$$\widetilde{D(\mathbf{r})} = (G^T \cdot G)^{-1} \cdot G^T \cdot B(\mathbf{r}). \quad (7)$$

In diffusion tensor imaging (DTI), it is assumed [4] that distribution of molecules undergoing diffusion is characterized by the conditional probability density function $p(\mathbf{r}|\mathbf{r}_0, \tau)$ given by the expression (4). Thus, D can be associated with an ellipsoid, which is a probability density isosurface of molecule diffusion. Since D is a symmetric positive definite second-rank tensor, it can be decomposed into eigenvectors (which form an orthogonal basis) and real eigenvalues [5]:

$$D = E \cdot \Lambda \cdot E^{-1}, \quad (8)$$

$$E = [e_1\ e_2\ e_3] \text{ и } \Lambda = \begin{bmatrix} \lambda_1 & 0 & 0 \\ 0 & \lambda_2 & 0 \\ 0 & 0 & \lambda_3 \end{bmatrix}. \quad (9)$$

WORKING WITH DIFFUSION MRI DATA

The development of methods and tools for working with diffusion MRI data involves a comprehensive consideration of several aspects.

In this section, the key questions are: "Why do we use diffusion weighted images? What capabilities do they have? What information can be obtained with their use along with other MRI modalities?"

DWI IN THE STUDY OF TUMOR PROCESSES

Due to processing of diffusion MRI data and analysis of their parameters (apparent diffusion coefficient (ADC), fractional anisotropy (FA), average diffusion coefficient, etc.) together with other MRI modalities available for a particular patient, it is possible to non-invasively:

1. Classify a process.

Central nervous system (CNS) lymphoma often exhibits a lower ADC [6–9] than other potentially similar formations on structural MRI, such as glial tumors, metastases, or infectious lesions.

Some of the most common brain tumors in children significantly differ in their diffusion properties, which can be useful in differential diagnosis. In particular, medulloblastomas tend to have a significantly lower ADC [10] than ependymomas or pilocytic astrocytomas.

In most cases, DWI makes it possible to distinguish an abscess from tumor necrosis (on structural MRI, the signals from them often mimic each other), since the ADC for purulent exudate is usually much lower than for necrosis [11].

2. Determine the tumor grade.

In the study [12], a statistically significant correlation was demonstrated between tumor cellularity and the minimum ADC, which was not detected in relation to T2w images. It was noted that the ADC for high-grade glial tumors ($(0.82–2.46) \cdot 10^{-3}$ mm^2/ s, the average ADC value = $(1.26 \pm 0.40) \cdot 10^{-3}$ mm^2/ s)) significantly exceeded the value for low-grade tumors ($(1.94 –3.31) \cdot 10^{-3}$ mm^2/ s, the average ADC value = $(2.7 \pm 0.7) \cdot 10^{-3}$ mm^2/ s).

3. Predict the course of the disease, its outcome, and a clinical response to treatment.

Since not all brain tumors respond to a particular therapy in the same way, early detection of treatment failures will allow for faster implementation of alternative treatment. It was shown that DWI is sensitive to tissue cellularity and, therefore, can potentially be used as a therapeutic biomarker [13]. For example, a method of functional diffusion mapping was proposed in [14]. It was calculated as an ADC change between the maps constructed upon admission of the patient for treatment (baseline) and at the current moment. Each voxel is mapped with one of 3 colors: blue voxels – a decrease in ADC, indicating an increase in cell density in the tumor; red voxels – an increase in ADC, indicating a decrease in cell density; green voxels – no significant change in the ADC. Thus, this method makes it possible to quantitatively assess the tumor response to treatment at runtime, provided that structural MRI cannot always reliably demonstrate this response.

4. Perform tractography.

In its simplest form, tractography can be interpreted as follows [15–17]: each voxel is characterized by one predominant fiber orientation and combines these local orientations to derive global trajectories. Mathematically, a set of local fiber orientations can be considered as a three-dimensional (3D) vector field, and global trajectories – as its streamlines [18–20]. A streamline is any curve that is tangential to the vector field along a path and can be represented as a three-dimensional spatial curve $\boldsymbol{r}(s)$, parameterized by arc length s. To align the streamline with the vector field, the tangent over the arc length s must be equal to the vector in the appropriate ratio:

$$\frac{d\boldsymbol{r}(s)}{ds} = \boldsymbol{v}[\boldsymbol{r}(s)], \quad (10)$$

where $\boldsymbol{r}(s)$ denotes the position along the streamline and **v** is the three-dimensional vector field.

The above-described equation is differential and can be solved as follows:

$$r(s) = \int_{s_0} \boldsymbol{v}[\boldsymbol{r}(s)]ds, \quad (11)$$

where $\boldsymbol{r}(\boldsymbol{s_0}) = \boldsymbol{r_0}$ represents the starting point of the streamline.

The above described streamline orientation is commonly called streamline reconstruction or tractography, and the resulting trajectories are called tracts or paths. A tractogram is a set of tracts reconstructed using tractography.

There are two different approaches in tractography: deterministic and probabilistic (there is also a global one [21–23], but its detailed consideration remains outside this article). With their help, it is possible to visualize various information [24, 25], such as brain tracts and connection maps, respectively. A lack of information about the error in the fiber tracking procedure is a significant limitation of deterministic tractography methods. To assess this uncertainty, probabilistic tractography algorithms create a large set of tracts (or a distribution of possible trajectories from each starting point). The results of probabilistic tractography are often presented in the form of quan-

titative maps showing the number of tracts that pass through a voxel, since it is assumed that the areas of the brain that are displayed with higher densities of the resulting trajectories have a higher probability of a connection with the starting point [26, 27].

DWI IN THE STIDY OF NON-TUMOR PROCESSES

The parameters of diffusion MRI can be considered as predictors of pathology long before it appears morphologically. For example, DTI allows to detect specific changes in the quantitative diffusion parameters of patients with functional pathologies, such as epilepsy, multiple sclerosis (MS), Parkinson's and Alzheimer's diseases, obsessive-compulsive disorder (OCD), etc.

According to the data of post-mortem studies, there is widespread involvement of the gray matter in the demyelinating process in MS. At the same time, some cortical tumors remain invisible on structural MRI (even using 3.0 T MRI scanners [28]). In a study [29], it was shown that the FA values for intracortical MS lesions are higher than for lesions in the gray matter. This self-contradictory discovery may actually reflect loss of dendrites within the lesion and activation of microglial cells. In another work [30], a relationship between T2 relaxation time and quantitative DTI data was investigated. MS lesions with longer times showed the most pronounced diffusion anomalies, which strongly correlated with a reduced content of myelin water. Taken together, these results support the idea that DTI is capable of detecting and assessing the severity of functionally significant tissue damage in MS at early stages.

It was shown that in the potentially epileptogenic areas [31], a decrease in FA and an increase in the average diffusion coefficient were observed. At the same time, tractography detected changes in the brain fibers responsible for memory and speech in patients with temporal lobe epilepsy.

The cingulum has long been known to be involved in the pathogenesis of OCD, but the results of its research are ambiguous. Studies on the left cingulum revealed both higher [32] and lower FA values compared to the control [33]. Other works [33; 34] demonstrated lower FA values in the right cingulum in patients with OCD. In addition to the data on the cingulum, high FA values were found in the inner capsule, corpus callosum [34; 35], and centrum semiovale [36]; low FA level was observed in the parietal lobe, supramarginal gyri, and left lingual gyrus in the occipital lobe [33]. The data described above are successfully used for functional stereotactic radiosurgery [37] (Fig. 1).

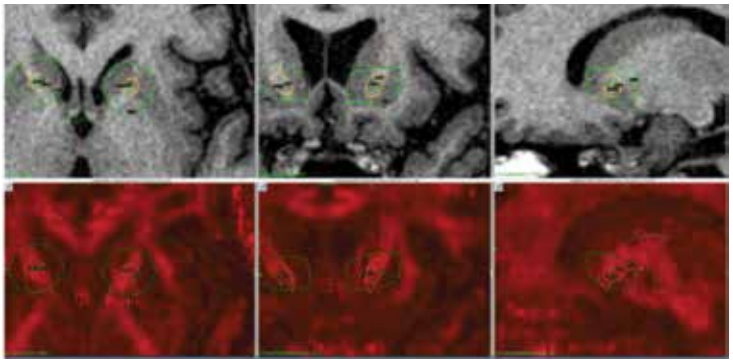

Fig. 1. Gamma Knife radiosurgery plan for a patient with obsessive-compulsive disorder: as a target, the inner capsule is chosen ((orange outline), prescribed radiation dose of 80 Gy along the 50% isodose line); inner green line – 140 Gy, yellow line – 80 Gy, outer green line – 15 Gy

RADIOSENSITIVITY OF THE BRAIN WHITE MATTER TRACTS

Another way of using diffusion weighted imaging relates to visualization of critical structures and optimization of the dose they receive during stereotactic radiosurgery. In modern clinical practice, we have limited recommendations on the tolerance doses for critical structures. If we discuss the effect of the dose on the brain, there is no differentiation of dose restrictions for the white matter, cerebral cortex, and various structures of the gray matter. The need for such differentiation and the need for visualizing and isolating tracts adjacent to or involved in a tumor and reducing the radiation dose applied to them are being discussed.

The study [38] demonstrated that with an increase in the radiation dose applied to the area of interest and time after the course of radiation therapy, the values of the coefficients of mean, axial (λ‖), and radial (λ⊥) diffusion significantly increased with a corresponding decrease in FA, which indicated changes in fibers and their radiosensitivity to therapeutic radiation doses. The changes were significant after 4–6 months or more (p <0.001). Hence, it can be concluded that when planning the irradiation of targets located in the vicinity of functional zones, negligence of adjacent white matter tracts is likely to result in neurocognitive impairments.

INSTRUMENTS FOR WORKING WITH DIFFUSION MRI DATA

The key questions discussed in this section are: "How to develop instruments for working with diffusion MRI data? What problems and limitations can be faced and how to solve them? What software is available today?"

Problems of working with diffusion MRI data:

1. Processing of ambiguous local geometries.

When using the tensor model for working with diffusion MRI data, it is impossible to distinguish at the voxel level such fiber configurations as crossing, kissing, bending, and fanning [39]. In this case, it may be necessary to use higher order diffusion models [40–47].

2. Reconstructions near the cortex.

Tracking fibers near the cortex and gyri is a challenging task [48, 49], since it is determined by large modeling errors in the local assessment of fiber orientation when approaching the gray matter. Higher order algorithms provide high quality assessment of fiber orientation in white matter voxels. However, along with this, they can give unreliable results in voxels partially containing gray matter. To solve this problem, it is necessary to use local models that take into account the presence of other types of tissues or microstructural compartments.

3. Spatial resolution.

Currently, acquisition of whole-brain DWI for routine use within a reasonable scan time is limited to 2 mm^3 spatial resolution. At the same time, it is obvious that in order to characterize the fine structures of the white matter and, in particular, the intricate structures of the cerebral cortex or small structures near the gray matter (nuclei, brain stem), higher spatial resolution is required. Increasing it is not a trivial task, since it is usually accompanied by either a significant decrease in the signal-to-noise ratio or a significant increase in the acquisition time.

4. Angular resolution.

Local orientation models fail to distinguish between two fiber populations, when the angle between them falls below a certain threshold. Such effects could potentially generate entirely artificial fibers. Despite the existence of such a term as high angular resolution diffusion imaging, angular resolution of DWI is rather limited. As a consequence, even with the most advanced high angular resolution diffusion imaging and advanced fiber orientation techniques, angles below 30° between fibers are rarely resolved.

5. False positives.

As shown in [50–52], due to the fact that different fiber configurations can lead to the same MRI signal in the voxel, a large number of false positive tracts and connections are generated. For 96 tractograms shown at the ISMRM 2015 Tractography Challenge by the 21st International Group, there were on average four false positives per a valid fiber.

6. Artifacts.

DWI, like any echo planar imaging, is characterized by a number of artifacts: physical hardware (magnetic susceptibility, eddy currents, gradient artifact, etc.) and artifacts associated with the object of the study (artifacts of movement, blood pulsations, chemical shift, fat suppression, etc.).

IMAGE DISTORTION CORRECTION

Before working with DWI, it is necessary to process the image, namely, to correct the distortions caused by the above-described artifacts. At the same time, new methods (both hardware and software) for dealing with them already exist and are constantly developing.

The most interesting is the correction method implemented in FSL toolbox (FMRIB, England). It is based on the choice of a covariance function that predicts the signal from voxels even with complex fiber configurations.

Diffusion MRI data (in each voxel) are obtained by measuring the signal after applying diffusion weighting (characterized by a b-factor and a unit-length vector **g** defining the direction). A complete diffusion protocol consists of multiple measurements in different gradient directions. Hence, the data can be viewed as a response variable (signal) obtained at the surface of the sphere.

Two important aspects should be noted: 1) the signal changes smoothly when the angle of the diffusion

weighting direction changes; 2) the signal is axially symmetric, that is, the signal along $\boldsymbol{g}$ is identical to the signal along -$\boldsymbol{g}$.

Since the diffusion signal is distributed over the sphere, the methods used in geostatistics can be used to work with it. One such method is kriging, it is a special case of the Gaussian process observed on the sphere. For these methods, covariance is often defined as a function of the angle θ between two vectors from the center of the sphere to x (observed points) and x' (points predicted in the absence of distortion). These vectors are easily represented as the $\boldsymbol{g}$-vectors described above. Two popular covariance functions that determine the relationship between observed points and predicted (sought) points in geostatistics are:

1) exponential model:

$$C(\theta) = e^{-\theta/a} \text{ for } 0 \le \theta \le \pi, \quad (12)$$

where a is the positive parameter of the scale;

2) spherical model

$$C(\theta) = \begin{cases} 1 - \frac{3\theta}{2a} + \frac{\theta^3}{2a^3} & \text{for } \theta \le a \\ 0 & \text{for } \theta \ge a \end{cases}, \quad (13)$$

where a is a positive parameter of the scale, which here defines the distance at which the covariance θ tends to zero.

SOFTWARE FOR WORKING WITH DWI

The process of working with diffusion images is divided into the following stages: pre-processing, including correction of artifacts and extraction of the brain mask, direct work with the image and visualization, namely, estimation of diffusion tensors, construction of maps for diffusion parameters and tracts, clustering, and then quantitative analysis. If we consider the whole variety of software that works with DWI, relying on the stages of working with it, we can distinguish several programs: AFNI (NIMH, USA), FSL (FMRIB, England), MRTrix (collaboration of a large number of institutions from different countries of the world), 3D Slicer (NIH, USA), Camino (University College London, England), TrackVis (MGH GCRC and NIMH, USA), etc. However, none of them covers the entire range of tasks. In addition, many software products developed for processing diffusion images involve writing and / or understanding of scripts, which implies a lot of manual work that is not transparent to non-programmers. At the moment, when planning radiation therapy, the function of diffusion MRI data processing is not available in commercial specialized software.

Therefore, the task of developing software that most fully covers the tasks of working with diffusion MRI data remains relevant.

DEVELOPMENT OF SELF-DESIGNED SOFTWARE

We are developing the MRDiffusion application in the standard C ++ language. The subject part has been moved to separate class libraries and can be used on various platforms. The current user interface is Windows 10. Forms are written in XAML. Graphics is generated using the DirecX environment. Open source math libraries are used for some computational tasks.

Using the interface, you can upload (Fig. 2) files obtained during MRI in DICOM with series of DTI, which will be displayed with the ability to select a specific series. It is convenient in terms of navigating through images and is effective in the work setting.

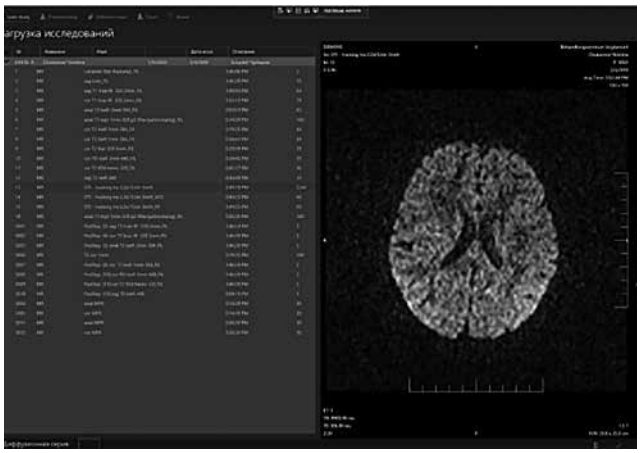

Fig. 2. Loading images into MRDiffusion

For further image processing, it is necessary to extract the brain mask, which is performed on images with a zero gradient, that is, on T2w (Fig. 3, *a*).

Using the application, it is possible to calculate such quantitative parameters as average diffusion and FA, presented in two versions: conventional and with color coding of directions (Fig. 3. *b*).

At the moment, tractography is implemented by a simple deterministic method – fiber assignment by continuous tracking (FACT). Its essence is as follows.

Path selection begins at the center of each voxel with an FA value above the predetermined threshold and continues parallel to the main diffusion direction. Black arrows (Fig. 4, *a*) indicate the diffusion tensor eigenvectors with the largest eigenvalue. At the point where the path crosses the voxel, the direction changes according to the new main direction. Iteratively

continuing such actions, restoration of the path will be interrupted when the conditions for stopping the algorithm occur: if the FA value in the voxel is less than the threshold or if the angle between the new and the old main directions of diffusion turns out to be higher than the predetermined angle threshold. The path is restored in both directions from the starting point: in the direction of the main vector and against it. Moreover, each piece of the tract has a color obtained by mixing red, green, and blue, which, in turn, indicate the main direction of diffusion in one direction or another (Fig. 4, *b*).

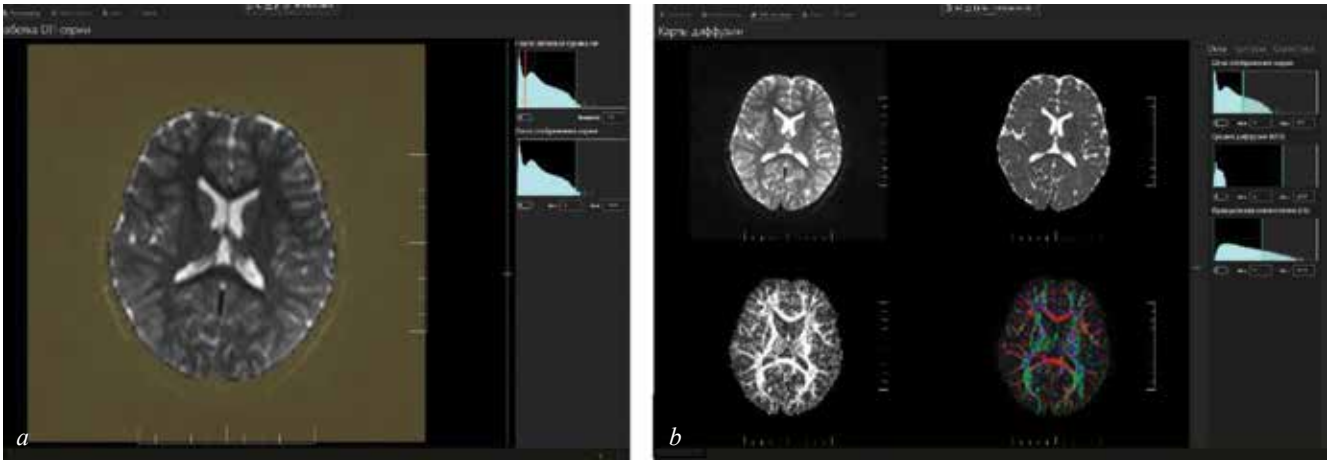

Fig. 3. Extraction of the brain mask (*a*); quantitative diffusion maps (*b*)

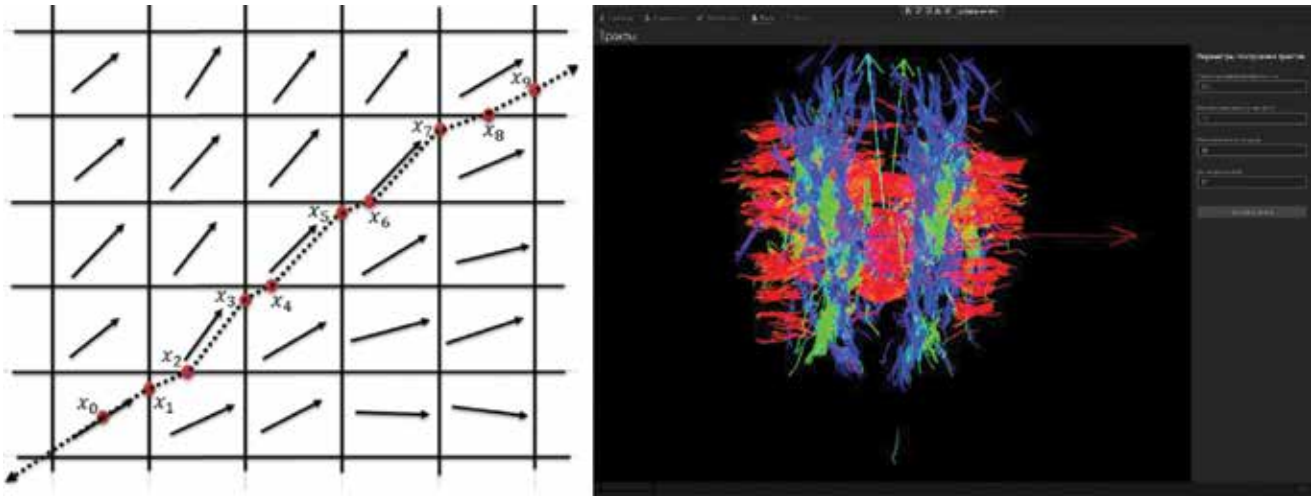

Fig. 4. Scheme of FACT algorithm (*a*), an example of FACT tractography (*b*)

CONCLUSION

Since its emergence in the mid-1990s, diffusion weighted MRI has been widely used in medical imaging for data processing and analysis, and especially in brain research. This is due to its unique capabilities (compared to other modalities), namely, the ability to quantitatively and qualitatively investigate tissue structure and function at the cellular level without the use of contrast agents or ionizing radiation. The most promising application of this technique, in addition to routine medical research, is its use in planning radiation therapy and neurosurgical operations and studying epilepsy, Alzheimer's and Parkinson's diseases, multiple sclerosis, and other disorders. The use of this technology in other areas is strongly limited by the ability to correctly interpret the results.

Diffusion weighted MRI of the brain is undoubtedly a promising non-invasive technology, but working with it is associated with a number of problems: 1) a

high probability of appearance of false positive fibers; 2) the impossibility of finding a difference and, as a consequence, a reliable reconstruction of intersecting, kissing, and merging fibers; 3) a lack of reproducibility of the result, dependence on the user; 4) the impossibility of displaying short tracts; 5) the instability of algorithms when working with pathology.

REFERENCES

1. Einstein A. Über die von der molecularkinetischen Theorie der Wärme geforderte Bewegung von in ruhenden Flüssigkeiten suspendierten Teilchen. An-nalen der Physik. 1905; 322 (8): 549–560.
2. Leemans A. Modeling and processing of diffusion tensor magnetic resonance images for improved analysis of brain connectivity. PhD thesis. University of Antwerp, Antwerpen, 2006.
3. Hashemi R., Bradley W., Lisanti C. MRI. The Basics. Lippincott Williams & Wilkins. Ph., 2004: 353.
4. Laun F., Fritzsche K., Kuder T., Stieltjes B. Introduction to the basic principles and techniques of diffusion-weighted imaging. *Radiology*. 2011; 51 (3):170–179. DOI: 10.1007/s00117-010-2057-y.
5. Basser P., Mattiello J., Le Bihan D. MR diffusion tensor spectroscopy and imaging. *Biophysical Journal*. 1994; 66 (1): 259–267. DOI: 10.1016/S0006-3495(94)80775-1.
6. Kitis O., Altay H., Calli C., Yunten N., Akalin T., Yurtseven T. Minimum apparent diffusion coefficients in the evaluation of brain tumors. *Eur. J. Radiol*. 2005; 55 (3): 393-400. DOI: 10.1016/j.ejrad.2005.02.004.
7. Yamasaki F., Kurisu K., Satoh K., Arita K., Sugiyama K., Ohtaki M. et al. Apparent diffusion coefficient of human brain tumors at MR imaging. *Radiology*. 2005; 235 (3): 985–991. DOI: 10.1148/RADIOL.2353031338.
8. Al-Okaili R., Krejza J., Woo J.H., Wolf R., O'Rourke D., Judy K. et al. Intraaxial brain masses: MR imaging-based diagnostic strategy – initial experience. *Radiology*. 2007; 243 (2): 539–550. DOI: 10.1148/radiol.2432060493.
9. Toh C., Castillo M., Wong A., Wei K., Wong H., Ng S. et al. Primary cerebral lymphoma and glioblastoma multiforme: differences in diffusion characteristics evaluated with diffusion tensor imaging. *AJNR Am. J. Neuroradiol*. 2008; 29 (3): 471–475. DOI: https://doi.org/10.3174/ajnr.A0872.
10. Wilke M., Eidenschink A., Muller-Weihrich S., Auer D. MR diffusion imaging and 1H spectroscopy in a child with medulloblastoma. A case report. *Acta Radiol.* 2001; 42 (1): 39–42.
11. Guzman R., Barth A., Lovblad K., El-Koussy M., Weis J., Schroth G. Use of diffusion-weighted magnetic resonance imaging in Diffusion Imaging in Brain Tumors differentiating purulent brain processes from cystic brain tumors. *J. Neurosurg*. 2002; 97 (5): 1101–1107. DOI: 10.3171/jns.2002.97.5.1101.
12. Sugahara T., Korogi Y., Kochi M., Ikushima I., Shigematu Y., Hirai T., Okuda T., Liang L., Ge Y., Komohara Y. et. al. Usefulness of diffusion-weighted MRI with echo-planar technique in the evaluation of cellularity in gliomas. *J. Magn. Reson. Imaging.* 1999; 9 (1): 53–60. DOI: 10.1002/(SICI)1522-2586(199901)9:1<53::AID-JMRI7>3.0.CO;2-2.
13. Schmainda K. Diffusion-weighted MRI as a biomarker for treatment response in glioma. *CNS Oncology*. 2012; 1 (2):169–180. DOI: 10.2217/cns.12.25.
14. Ellingson B., Malkin M., Rand S. et al. Validation of functional diffusion maps (fDMs) as a biomarker for human glioma cellularity. *J. Magn. Reson. Imaging*. 2010; 31 (3): 538–548. DOI: 10.1002/jmri.22068.
15. Mori S., Zijl P. Fiber tracking: Principles and strategies – A technical review. *NMR in Biomedicine.* 2002; 15 (7-8): 468–480. DOI: 10.1002/nbm.781.
16. Lazar M. Mapping brain anatomical connectivity using white matter tractography. *NMR Biomed.* 2010; 23 (7): 821–835. DOI: 10.1002/nbm.1579.
17. Wasserthal J., Neher P., Maier-Hein K. Tract orientation mapping for bundle-specific tractography. Springer, 2018. DOI: 10.1007/978-3-030-00931-1_5.
18. Conturo T., Lori N., Cull T. et al. Tracking neuronal fiber pathways in the living human brain. *Proc. Natl. Acad. Sci.* 1999; 96 (18): 10422–10427. DOI: 10.1073/pnas.96.18.10422.
19. Mori S., Crain B.J., Chacko V.P., van Zijl P.C. Three-dimensional tracking of axonal projections in the brain by magnetic resonance imaging. *Ann. Neurol.* 1999; 45 (2): 265–269. DOI: 10.1002/1531-8249(199902)45:2<265::aid-ana21>3.0.co;2-3.
20. Basser P., Pajevic S., Pierpaoli C. et al. In vivo fiber tractography using DT-MRI data. *Magn. Reson. Med.* 2000; 44 (4): 625–632. DOI: 10.1002/1522-2594(200010)44:4<625::aid-mrm17>3.0.co;2-o.
21. Reisert M., Mader I., Anastasopoulos C. et al. Global fiber reconstruction becomes practical. *Neuroimage*. 2011; 54 (2): 955–962. DOI: 10.1016/j.neuroimage.2010.09.016.
22. Mangin J-F., Fillard P., Cointepas Y. et al. Toward global tractography. *Neuroimage*. 2013; 80: 290–296. DOI: 10.1016/j.neuroimage.2013.04.009.
23. Christiaens D., Reisert M., Dhollander T. et al. Global tractography of multi-shell diffusion-weighted imaging data using a multi-issue model. *Neuroimage*. 2015; 123: 89–101. DOI: 10.1016/j.neuroimage.2015.08.008.
24. Behrens T., Woolrich M., Jenkinson M. et al. Characterization and propagation of uncertainty in diffusion-weighted MR imaging. *Magn. Reson. Med.* 2003; 50 (5): 1077–1088. DOI: 10.1002/MRM.10609.
25. Behrens T., Berg H., Jbabdi S., Rushworth M., Woolrich M. Probabilistic diffusion tractography with multiple fibre orientations: what can we gain? *Neuroimage.* 2007; 34 (1): 144–155. DOI: 10.1016/j.neuroimage.2006.09.018.
26. Parker G., Alexander D. Probabilistic anatomical connectivity derived from the microscopic persistent angular structure of cerebral tissue. *Philos. Trans. R. Soc. Lond. B Biol. Sci*. 2005; 360 (1457): 893–902. DOI: 10.1098/rstb.2005.1639.
27. Parker G., Haroon H., Wheeler-Kingshott C. A Framework for a streamline-based probabilistic index of connectivity (PICo) using a structural interpretation of MRI diffusion measurements. *J. Magn. Reson. Imaging*. 2003; 18 (2): 242–254. DOI: 10.1002/jmri.10350.
28. Polman C., Reingold S., Banwell B. et al. Diagnostic criteria for multiple sclerosis: 2010 revisions to the McDonald criteria. *Annals of Neurology*. 2011; 69 (2): 292–302. DOI: 10.1002/ana.22366.

29. Poonawalla A., Hasan K., Gupta R., Ahn C., Nelson F., Wolinsky J., Narayana P. Diffusion-tensor MR imaging of cortical lesions in multiple sclerosis: initial findings. *Radiology.* 2008; 246(3): 880–886. DOI: 10.1148/radiol.2463070486.
30. Kolind S., Laule C., Vavasour I., Li D.K., Traboulsee A., Mädler B., Moore G., Mackay A. Complementary information from multi-exponential T2 relaxation and diffusion tensor imaging reveals differences between multiple sclerosis lesions. *Neuroimage*. 2008; 40(1): 77–85. DOI: 10.1016/j.neuroimage.2007.11.033.
31. Hugg J., Butterworth E., Kuzniecky R. Diffusion mapping applied to mesial temporal lobe epilepsy: preliminary observations. *Neurology*. 1999; 53(1): 173 – 176. DOI: 10.1212/wnl.53.1.173.
32. Cannistraro P., Makris N., Howard J., Wedig M., Hodge S., Wilhelm S., Kennedy D., Rauch S. A diffusion tensor imaging study of white matter in obsessive-compulsive disorder. *Depress Anxiety*. 2007; 24(6): 440–446. DOI: 10.1002/da.20246.
33. Szeszko P., Ardekani B., Ashtari M., Malhotra A., Robinson D., Bilder R., Lim K. White matter abnormalities in obsessive-compulsive disorder: a diffusion tensor imaging study. *Arch. Gen Psychiatry*. 2005; 62(7): 782–790. DOI: 10.1001/archpsyc.62.7.782.
34. Cannistraro P., Makris N., Howard J., Wedig M., Hodge S., Wilhelm S. et al. A diffusion tensor imaging study of white matter in obsessive-compulsive disorder. *Depress Anxiety.* 2006; 24: 440–446. DOI: 10.1007/978-1-59745-495-7_3.
35. Yoo S., Jang J., Shin Y., Kim D., Park H., Moon W., Chung E., Lee J., Kim I., Kim S., Kwon J. White matter abnormalities in drug-naive patients with obsessive-compulsive disorder: a diffusion tensor study before and after citalopram treatment. *Acta Psychiatr. Scand*. 2007; 116 (3): 211–219. DOI: 10.1111/j.1600-0447.2007.01046.x.
36. Nakamae T., Narumoto J., Shibata K., Matsumoto R., Kitabayashi Y., Yoshida T., Yamada K., Nishimura T., Fukui K. Alteration of fractional anisotropy and apparent diffusion coefficient in obsessive-compulsive disorder: a diffusion tensor imaging study. *Prog. Neuropsychopharmacol. Biol. Psychiatry.* 2008; 32(5): 1221–1226. DOI: 10.1016/j.pnpbp.2008.03.010.
37. Gavin C., Ian Sabin H. Stereotactic diffusion tensor imaging tractography for Gamma Knife radiosurgery. *J. Neurosurgery*. 2016; 125 (1):139–146. DOI: 10.3171/2016.8.GKS161032.
38. Connor M., Karunamuni R., McDonald C., White N., Pettersson N., Moiseenko V., Seibert T., Marshall D., Cervino L., Bartsch H., Kuperman J., Murzin V., Krishnan A. et al. Dose-dependent white matter damage after brain radiotherapy. *Radiothion. Oncol*. 2016; 121 (2): 209–216. DOI: 10.1016/j.radonc.2016.10.003.
39. Tournier J.-D., Calamante F., Connelly A. MRtrix: diffusion tractography in crossing fiber regions. *Int. J. Imaging Syst. Technol.* 2012; 22: 53–66. DOI: 10.1002/IMA.22005.
40. Wedeen V., Hagmann P., Tseng W. Mapping Complex Tissue Architecture with Diffusion Spectrum Magnetic Resonance Imaging. *Magnetic Resonance in Medicine*. 2005; 54 (6): 1377–1386. DOI: 10.1002/MRM.20642.
41. Campbell J., Siddiqi K., Rymar V. Flow-based fiber tracking with diffusion tensor and q-ball data: validation and comparison to principal diffusion direction techniques. *Neuroimag*e. 2005; 27 (4): 725–736. DOI: 10.1016/j.neuroimage.2005.05.014.
42. Tuch, D. Q-ball imaging. *Magn. Reson. Med*. 2004; 52 (6): 1358–1372. DOI: 10.1002/mrm.20279.
43. Assaf Y., Basser P. Composite hindered and restricted model of diffusion (CHARMED) MR imaging of the human brain. *Neuroimage*. 2005; 27 (1): 48–58. DOI: 10.1016/j.neuroimage.2005.03.042.
44. Özarslan E., Shepherd T., Vemuri B. et al. Resolution of complex tissue microarchitecture using the diffusion orientation transform (DOT). *Neuroimage* 2006; 31 (3): 1086–1103. DOI: 10.1016/j.neuroimage.2006.01.024.
45. Liu C., Bammer R., Acar B. et al. Characterizing non-Gaussian diffusion by using generalized diffusion tensors. *Magn. Reson. Med*. 2004; 51 (5): 924–937. DOI: 10.1002/mrm.20071
46. Tournier J.-D., Calamante F., Gadian D. et al. Direct estimation of the fiber orientation density function from diffusion-weighted MRI data using spherical deconvolution. *Neuroimage*. 2004; 23 (3): 1176–1185. DOI: 10.1016/j.neuroimage.2004.07.037.
47. Tournier J.-D., Calamante F., Connelly A. Robust determination of the fibre orientation distribution in diffusion MRI: non-negativity constrained super resolved spherical deconvolution. *Neuroimage.* 2007; 35 (4): 1459–1472. DOI: 10.1016/j.neuroimage.2007.02.016.
48. Jbabdi S., Johansen-Berg H. Tractography: where do we go from here? *Brain Connect*. 2011; 1 (3): 169–183. DOI: 10.1089/brain.2011.0033.
49. Thomas C., Ye F., Irfanoglu M. et al. Anatomical accuracy of brain connections derived from diffusion MRI tractography is inherently limited. *Proc. Natl. Acad. Sci. USA*. 2014; 111 (46): 16574–16579. DOI: 10.1073/pnas.1405672111.
50. Maier-Hein K., Neher P., Houde J.-C. et al. Tractography-based connectomes are dominated by false-positive connections. *bioRxiv*. 2016; 1: 84137. DOI: 10.1101/084137.
51. Fillard P., Descoteaux M., Goh A., Gouttard S., Jeurissen B., Malcolm J., Ramirez-Manzanares A., Reisert M., Sakaie K., Tensaouti F. et al. Quantitative evaluation of 10 tractography algorithms on a realistic diffusion MR phantom. *Neuroimage*. 2011; 56 (1): 220–234. DOI: 10.1016/j.neuroimage.2011.01.032.
52. Maier-Hein K., Neher P., Houde J.., Côté M., Garyfallidis E., Zhong J., Chamberland M., Yeh F., Lin Y., Descoteaux M. et al. The challenge of mapping the human connectome based on diffusion tractography. *Nature Communications*. 2017; 8 (1): 1349. DOI: 10.1038/s41467-017-01285-x.

Authors information

Urazova Ksenia A., Engineer-Physicist, Department of Radiosurgery and Radiotherapy, N.N. Burdenko National Scientific and Practical Center for Neurosurgery; Post-Graduate Student, Department of Physics of Accelerators and Radiation Medicine, M.V. Lomonosov Moscow State University, Moscow, Russian Federation. ORCID 0000-0002-7725-5090.

Gorlachev Gennady E., Cand. Sci. (Physics and Mathematics), Senior Researcher, Clinical Dosimetry Group, N.N. Blokhin National Medical Research Center of Oncology, Moscow, Russian Federation. ORCID 0000-0003-4386-4223.

Chernyaev Alexander P., Dr. Sci. (Physics and Mathematics), Professor, Head of the Department of Accelerator Physics and Radiation Medicine, M.V. Lomonosov Moscow State University, Moscow, Russian Federation. ORCID 0000-0001-5250-046X.

Golanov Andrey V., Dr. Sci. (Med.), Professor, Corresponding Member of RAS, Head of the Department of Radiosurgery and Radiotherapy, N.N. Burdenko National Scientific and Practical Center for Neurosurgery, Moscow, Russian Federation. ORCID 0000-0002-0976-4547.

(✉) **Urazova Ksenia A.,** e-mail: kurazova@nsi.ru.

Received 25.08.2020

Accepted 28.12.2020